
Unsupervised Temperature Scaling: Post-Processing Unsupervised Calibration of Deep Models Decisions

Azadeh Sadat Mozafari¹ Hugo Siqueira Gomes¹ Wilson Leão² Christian Gagné¹

Abstract

Great performances of deep learning are undeniable, with impressive results on wide range of tasks. However, the output confidence of these models is usually not well calibrated, which can be an issue for applications where confidence on the decisions is central to bring trust and reliability (e.g., autonomous driving or medical diagnosis). For models using softmax at the last layer, Temperature Scaling (TS) is a state-of-the-art calibration method, with low time and memory complexity as well as demonstrated effectiveness. TS relies on a T parameter to rescale and calibrate values of the softmax layer, using a labelled dataset to determine the value of that parameter. We are proposing an Unsupervised Temperature Scaling (UTS) approach, which does not depend on labelled samples to calibrate the model, allowing, for example, using a part of test samples for calibrating the pre-trained model before going into inference mode. We provide theoretical justifications for UTS and assess its effectiveness on the wide range of deep models and datasets. We also demonstrate calibration results of UTS on skin lesion detection, a problem where a well-calibrated output can play an important role for accurate decision-making.

1. Introduction

Deep Neural Networks (DNNs) demonstrated dramatically accurate results for challenging tasks (He et al., 2016; Simonyan & Zisserman, 2014; Graves et al., 2013; Bar et al., 2015). However, in real-world decision-making applications, accuracy is not the only element considered, the confidence of the network being also essential for having a secure and reliable system. In DNNs, confidence usually

corresponds to the output of a softmax layer, which is typically interpreted as the likeliness (probability) of different class occurrence. Most of the time, this value is far from the true probability of each class occurrence, with a tendency to get overconfident (i.e., output of one class close to 1 and other classes close to 0). In such case, we usually consider the DNN not to be well-calibrated.

Calibration in DNNs is a recent challenge in machine learning community as it is not an issue for shallow neural networks (Niculescu-Mizil & Caruana, 2005). Gua et al. (Guo et al., 2017) has studied the role of different parameters which makes a neural network uncalibrated. They show a deep network optimized with the Negative Log Likelihood (NLL) loss can reach higher accuracy when overfitting the NLL. However, the side effect of overfitting according to NLL is to make the network overconfident.

Having calibrated network is important for real-world applications. In a self-driving car (Bojarski et al., 2016) deciding about transferring the control of the car to the human observer is taken regarding to the confidence of the detected objects. In medical care systems (Jiang et al., 2011), the deadly diseases can be missed when they are wrongly detected as a non-problematic case with high confidence. Calibration adds more information to the system which consequences reliability. Calibration methods for DNNs are widely investigated in recent literature and can be categorized into two main directions: 1-probabilistic approach 2-measure-based approach. Probabilistic approaches generally include approximated Bayesian formalism (MacKay, 1992; Neal, 2012; Louizos & Welling, 2016; Gal & Ghahramani, 2016; Lakshminarayanan et al., 2017). In practice, the quality of predictive uncertainty in Bayesian-based methods relies heavily on the accuracy of sampling approximation and correctly estimated prior distribution and they suffer from time and memory complexity.

Comparatively, measure-based approach are more easy to use. They are generally post-processing methods that do not need to retrain the network to make it calibrated. They apply a function on the logit layer of the network and fine-tune the parameters of that function by minimizing a calibration measure as a loss function. Guo et al. (Guo et al., 2017) have summarized and compared several famous measure-based

¹Computer Vision and Systems Laboratory, Université Laval, Quebec City, Canada ²Petrobras, Brazil. Correspondence to: Azadeh Sadat Mozafari <azadeh-sadat.mozafari.1@ulaval.ca>.

calibration methods such as Temperature, Matrix, Vector Scaling (Platt et al., 1999), Histogram Binning (Zadrozny & Elkan, 2001), Isotonic Regression (Zadrozny & Elkan, 2002) and Baysian Binning into Quantiles (Naeini et al., 2015).

Temperature Scaling (TS) (Guo et al., 2017) is the state-of-the-art measure-based approach that comparing to the others, achieves better calibration with minimum computational complexity (optimizing only one parameter T to soften the softmax) which makes it the most appealing method in practice. It also preserves the accuracy rate of the network that can be degraded during the calibration phase. In TS, the best T parameter is found by minimizing Negative Log Likelihood (NLL) loss respecting to T on small-size validation set. In real scenarios, generally a pre-trained network is needed to be calibrated by gathering a set of labeled samples. Generally, labeling is a costly procedure. Therefore, if there was a possibility to calibrated the model with the part of the test samples it would be an interesting post-processing calibration solution.

Contribution: In this paper, we propose a new TS family method which is called Unsupervised Temperature Scaling (UTS) to calibrate the network without accessing to labels of the samples. Comparing to TS algorithm, UTS preserves the time and memory complexity advantage of classic TS as well as intact accuracy while it is independent of the labels of the samples for calibration.

2. Problem Setting

In this section, we set up the problem, notations and introduce NLL (Friedman et al., 2001) as a calibration measures.

Assumptions: We assume to have access to a pre-trained deep model $D(\cdot)$ with the ability of detecting K different classes. $D(\cdot)$ is trained on samples generated from distribution function $Q(\mathbf{x}, y)$. We also have access to test data with the same distribution that we select N number of samples of this test set as the validation set $\mathcal{V} = \{\mathbf{x}_i\}_{i=1}^N$ for calibration. For each sample \mathbf{x}_i , there exist $\mathbf{h}_i = [h_i^1, h_i^2, \dots, h_i^K]^\top$ which is the logit layer. $D(\mathbf{x}_i) = (\hat{y}_i, S_{y=\hat{y}_i}(\mathbf{x}_i))$ defines that the network $D(\cdot)$ detects label \hat{y}_i for input sample \mathbf{x}_i and confidence $S_{y=\hat{y}_i}(\mathbf{x}_i)$. $S_y(\mathbf{x}) = \exp(h_i^y) / \sum_{j=1}^K \exp(h_i^j)$ is the softmax output function of the model that here is interpreted as the confidence.

Goal: The objective is to re-scale \mathbf{h}_i with parameter T in order to minimize calibration error of the model.

2.1. Negative Log Likelihood (NLL)

When the network is calibrated, the softmax output layer is indicating the true conditional distribution $Q(y|\mathbf{x})$. To measure the calibration, the amount of similarity between $S_y(\mathbf{x})$ and $Q(y|\mathbf{x})$ functions will be computed. As $Q(y|\mathbf{x})$

distribution function is not available and only a bunch of generated samples from it is available, in this case, Gibbs inequality can help us to find the similarity between two distributions. Gibbs inequality is defined as Eq. (1) for any arbitrary distribution function $P(y|\mathbf{x})$:

$$-\mathbb{E}_{Q(\mathbf{x}, y)}[\log(Q(y|\mathbf{x}))] \leq -\mathbb{E}_{Q(\mathbf{x}, y)}[\log(P(y|\mathbf{x}))], \quad (1)$$

where \mathbb{E} is the expected value function. The minimum of $-\mathbb{E}_{Q(\mathbf{x}, y)}[\log P(y|\mathbf{x})]$ happens when $P(y|\mathbf{x})$ is equal to $Q(y|\mathbf{x})$. NLL is defined as the empirical estimation of $-\mathbb{E}_{Q(\mathbf{x}, y)}[\log P(y|\mathbf{x})]$ which in deep neural networks is rephrased with distribution function $S_y(\mathbf{x})$ as:

$$\text{NLL} = - \sum_{(\mathbf{x}_i, y_i)} \log(S_{y=y_i}(\mathbf{x}_i)), \quad (\mathbf{x}_i, y_i) \sim Q(\mathbf{x}, y). \quad (2)$$

To minimize calibration error, NLL will be minimized respecting to the parameters that fine-tune $S_y(\mathbf{x})$ function. This is equal to minimize the distance between DNN output confidence and true distribution $Q(y|\mathbf{x})$.

3. Temperature Scaling (TS)

TS previously is applied for calibration (Guo et al., 2017), distilling the knowledge (Hinton et al., 2015) and enhancing the output of DNNs for better discrimination between the in and out distribution samples (Liang et al., 2017). TS is a post-processing approach which rescales the logit layer of a deep model by parameter T that is called temperature. TS is used to soften the output of the softmax layer and makes it more calibrated. The best value of T will be obtained by minimizing NLL loss function respecting to T conditioned by $T > 0$ on small set $\mathcal{T} = (\mathbf{x}_i, y_i) \sim Q(\mathbf{x}, y)$ as defined in Eq. (3):

$$T^* = \arg \min_T \left(- \sum_{i=1}^N \log(S_{y=y_i}(\mathbf{x}_i, T)) \right) \quad (3)$$

$$s.t : T > 0, \quad (\mathbf{x}_i, y_i) \in \mathcal{T},$$

where $S_{y=y_i}(\mathbf{x}_i, T) = \exp(\frac{h_i^{y_i}}{T}) / \sum_{j=1}^K \exp(\frac{h_i^j}{T})$, is the softened version of softmax by applying parameter T . TS has the minimum time and memory complexity among calibration approaches as it only optimizes one parameter T on small validation set. Having only one parameter helps TS not only to be efficient and practical but also not to get over-fitted to NLL loss function when it is optimized on small validation set \mathcal{T} . TS also keeps the accuracy intact during the calibration which can be an important feature when there is a risk of accuracy drop because of calibration.

4. Unsupervised Temperature Scaling (UTS)

In this section, we explain our proposed approach that is called UTS. UTS is the unsupervised version of TS. It mini-

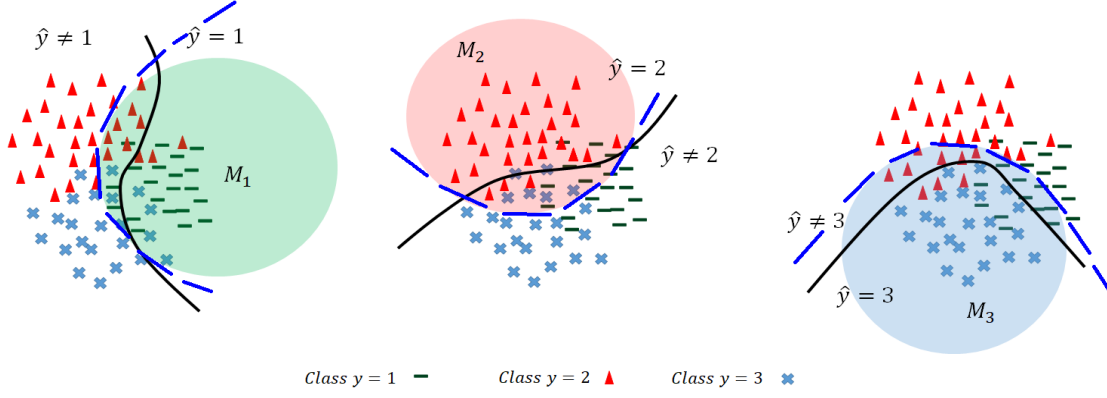


Figure 1. M_k subset division for a three class classification problem. The samples generated from distribution $Q(\mathbf{x}, y = k)$ are located in colored region of M_k where $S_{y=k}(\mathbf{x}_i) \geq \theta_k$. The dashed blue line shows the boundary of $S_{y=k}(\mathbf{x}) = \theta_k$ and the black continuous line shows the decision boundary which discriminates sample based on label prediction $\hat{y} = k$ or $\hat{y} \neq k$.

minimizes NLL respecting to T parameter for each class distribution instead of the total data distribution. This class-oriented distribution matching helps UTS to get rid of the true label of the samples. To estimate each class distribution, UTS minimizes NLL loss of $S_{y=k}(x)$ respecting to T , on the samples supposed to be generated from $Q(\mathbf{x}, y = k)$. The UTS loss function is proposed in Eq. (4):

$$\mathcal{L}_{UTS} = \sum_{k=1}^K \sum_{(\mathbf{x}_i) \in M_k} -\log(S_{y=k}(\mathbf{x}_i, T)), \quad (4)$$

$$T^* = \arg \min_T (\mathcal{L}_{UTS}), \quad s.t : T > 0,$$

M_k is the samples generated from the $Q(\mathbf{x}, y = k)$. Generally the samples that have true label $y = k$ belong to M_k . However UTS does not have access to the true labels of the samples. In this case, UTS uses the output of the classifier with this assumption that the samples which have bigger softmax value for $S_{y=k}(\mathbf{x})$ is more probable to belong to class k distribution. Formally M_k is defined as:

$$M_k = \{(\mathbf{x}_i) \mid S_{y=k}(\mathbf{x}_i) \geq \theta_k, \quad \mathbf{x}_i \in \mathcal{V}\} \quad (5)$$

θ_k is a threshold which is defined for each class k . We will explain how to select them in section 4.2. The samples of M_k fall into two conditions: 1- they correctly classified as $\hat{y} = k$ and 2- They are misclassified. If they are correctly classified, then they are generated from $Q(\mathbf{x}, y = k)$. If they are misclassified, we will show in section 4.1 that if these samples are selected from near to the decision boundary region, therefore they still can be used as the samples generated from distribution $Q(\mathbf{x}, y = k)$. Accordingly, we will define θ_k for each class k that only selects the misclassified samples which are located near to the decision boundary. Figure 1 shows the samples selected for M_k in the case of three class classification problem.

4.1. Analyzing the samples' distribution located near to the decision boundary

For the samples located near to the decision boundary of classifier k that discriminates class k samples from $\neq k$ samples, we have $Q(y = k|\mathbf{x}) \simeq Q(y \neq k|\mathbf{x})$. From the Bayesian Theorem we can define the distribution relation between two classes' samples:

$$Q(\mathbf{x}, y = k) = \frac{Q(y = k|\mathbf{x})}{Q(y \neq k|\mathbf{x})} Q(\mathbf{x}, y \neq k) \quad (6)$$

Therefore, for the sample near to the decision boundary, as $Q(y = k|\mathbf{x}) \simeq Q(y \neq k|\mathbf{x})$ they can be used as the samples generated from distributions $Q(\mathbf{x}, y = k)$ or $Q(\mathbf{x}, y \neq k)$ interchangeably.

4.2. How to select threshold θ_k

As explained in section 4, the group of samples that are misclassified as $\hat{y} \neq k$ should be near to the decision boundary that could be taken as the samples generated from $Q(\mathbf{x}, y = k)$. For the samples in this group, we assume as much as the softmax output $S_{y=k}(\mathbf{x})$ is bigger it means the sample is more close to the decision boundary of class k . Therefore to be sure that the samples are located near enough to the decision boundary, we define θ_k as follow:

$$\theta_k = \text{mean}(S_{y=k}(\mathbf{x}_i)) + \text{std}(S_{y=k}(\mathbf{x}_i)) \quad (7)$$

Where $D(\mathbf{x}_i) = (\hat{y} \neq k, S_{y=\hat{y}}(\mathbf{x}_i))$. Eq.(7) is the simple criteria to select samples with bigger confidence value depending on the confidence distribution. However how to find θ_k more precisely can be considered as the future work.

Table 1. The results of calibration for UTS vs. TS and uncalibrated models for variation of datasets and models. We report the results for two different calibration measures NLL and ECE (explanation of ECE is given in Appendix, section A). The smaller means better calibration. We also report the T values for TS and UTS to show a small change in T can bring significant improvement in calibration.

Model	Dataset	Uncalibrated	Uncalibrated		TS			UTS		
		TS, UTS	NLL	ECE %	NLL	ECE	T_{TS}	NLL	ECE	T_{TS}
DenseNet40	CIFAR10	92.61%	0.286	4.089	0.234	3.241	2.505	0.221	0.773	1.899
DenseNet40	CIFAR100	71.73%	1.088	8.456	1.000	1.148	1.450	1.001	1.945	1.493
DenseNet100	CIFAR10	95.06%	0.199	2.618	0.156	0.594	1.801	0.171	3.180	2.489
DenseNet100	CIFAR100	76.21%	1.119	11.969	0.886	4.742	2.178	0.878	2.766	1.694
DenseNet100	SVHN	95.72%	0.181	1.630	0.164	0.615	1.407	0.162	1.074	1.552
ResNet110	CIFAR10	93.71%	0.312	4.343	0.228	4.298	2.960	0.207	1.465	2.009
ResNet110	CIFAR100	70.31%	1.248	12.752	1.051	1.804	1.801	1.055	2.796	1.562
ResNet110	SVHN	96.06%	0.209	2.697	0.158	1.552	2.090	0.152	0.550	1.758
WideResNet32	CIFAR100	75.41%	1.166	13.406	0.909	4.096	2.243	0.905	4.872	1.651
LeNet 5	MNIST	99.03%	0.105	0.727	0.061	0.674	1.645	0.043	0.584	1.857
VGG16	CIFAR10	92.09%	0.427	5.99	0.301	6.015	3.229	0.268	1.675	2.671

5. Experimental Results

We investigate the effectiveness of UTS in comparison to TS on a wide range of different model-datasets. In all experiments, we divide randomly the test data into 20% of the validation set and the rest as the test dataset to report the results on. For TS we use the labeled data while for UTS we ignored the labels of the samples and consider them as unlabeled.

Datasets: To investigate the validity of UTS, we test the methods on CIFAR-10 (Krizhevsky & Hinton, 2009), CIFAR-100 (Krizhevsky & Hinton, 2009), SVHN (Netzer et al., 2011), and MNIST (LeCun et al., 1998b). For the calibration application we use data extracted from the “ISIC 2018: Skin Lesion Analysis Towards Melanoma Detection” grand challenge datasets (Tschandl et al., 2018; Codella et al., 2017) that contains images of 7 different skin lesion types.

Models: We try wide range of different state-of-the-art deep convolutional networks with variations in depth. The selected DNNs are Resnet (He et al., 2016), WideResnet (Zagoruyko & Komodakis, 2016), DenseNet (Iandola et al., 2014), LeNet (LeCun et al., 1998a), and VGG (Simonyan & Zisserman, 2014). We use the data pre-processing, training procedures and hyper-parameters as described in each paper.

5.1. Results for Different Model-Datasets

Table 1, compares the calibration result of UTS to TS. Both methods keeps the accuracy unchanged before and after calibration which is the positive points of the TS family methods. UTS improves the calibration in several cases better than TS and always better than uncalibrated model. It shows having access to more samples generated not accurately from a distribution helps more to find optimal temperature value T for calibration comparing to less samples but exactly generated from that distribution.

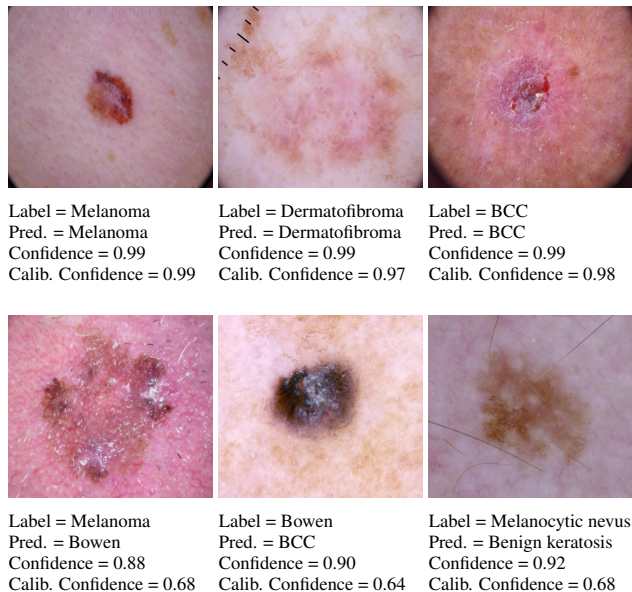


Figure 2. Confidence of skin anomaly detection system before and after calibration with UTS. UTS decreases the confidence of misclassified samples while keeps the confidence of correctly classified samples almost high.

5.2. Calibration Application: Skin Lesion Detection

In this section, we demonstrates the role of UTS for calibrating a real application where labeling is an expensive task. We use ISIC dataset (Tschandl et al., 2018; Codella et al., 2017) and trained ResNet152 for detecting 7 different skin lesions with accuracy 88.02%. More implementation details and results are provided in Appendix, sections B and C, respectively. Figure 2 shows the confidence of the model before and after calibrating the model with UTS for correctly classified and misclassified samples. Before calibration, the confidence of the system for both groups is high while after calibration the confidence of misclassified samples drops.

References

- Bar, Y., Diamant, I., Wolf, L., Lieberman, S., Konen, E., and Greenspan, H. Chest pathology detection using deep learning with non-medical training. In *ISBI*, pp. 294–297. Citeseer, 2015.
- Bojarski, M., Del Testa, D., Dworakowski, D., Firner, B., Flepp, B., Goyal, P., Jackel, L. D., Monfort, M., Muller, U., Zhang, J., et al. End to end learning for self-driving cars. *arXiv preprint arXiv:1604.07316*, 2016.
- Codella, N. C. F., Gutman, D., Celebi, M. E., Helba, B., Marchetti, M. A., Dusza, S. W., Kallou, A., Liopyris, K., Mishra, N. K., Kittler, H., and Halpern, A. Skin lesion analysis toward melanoma detection: A challenge at the 2017 international symposium on biomedical imaging (isbi), hosted by the international skin imaging collaboration (ISIC). *CoRR*, abs/1710.05006, 2017. URL <http://arxiv.org/abs/1710.05006>.
- Friedman, J., Hastie, T., and Tibshirani, R. *The elements of statistical learning*, volume 1. Springer series in statistics New York, 2001.
- Gal, Y. and Ghahramani, Z. Dropout as a bayesian approximation: Representing model uncertainty in deep learning. In *international conference on machine learning*, pp. 1050–1059, 2016.
- Graves, A., Mohamed, A.-r., and Hinton, G. Speech recognition with deep recurrent neural networks. In *Acoustics, speech and signal processing (icassp), 2013 IEEE international conference on*, pp. 6645–6649. IEEE, 2013.
- Guo, C., Pleiss, G., Sun, Y., and Weinberger, K. Q. On calibration of modern neural networks. *arXiv preprint arXiv:1706.04599*, 2017.
- He, K., Zhang, X., Ren, S., and Sun, J. Deep residual learning for image recognition. In *Proceedings of the IEEE conference on computer vision and pattern recognition*, pp. 770–778, 2016.
- Hinton, G., Vinyals, O., and Dean, J. Distilling the knowledge in a neural network. *arXiv preprint arXiv:1503.02531*, 2015.
- Iandola, F., Moskewicz, M., Karayev, S., Girshick, R., Darrell, T., and Keutzer, K. Densenet: Implementing efficient convnet descriptor pyramids. *arXiv preprint arXiv:1404.1869*, 2014.
- Jiang, X., Osl, M., Kim, J., and Ohno-Machado, L. Calibrating predictive model estimates to support personalized medicine. *Journal of the American Medical Informatics Association*, 19(2):263–274, 2011.
- Krizhevsky, A. and Hinton, G. Learning multiple layers of features from tiny images. Technical report, Citeseer, 2009.
- Lakshminarayanan, B., Pritzel, A., and Blundell, C. Simple and scalable predictive uncertainty estimation using deep ensembles. In *Advances in Neural Information Processing Systems*, pp. 6402–6413, 2017.
- LeCun, Y., Bottou, L., Bengio, Y., Haffner, P., et al. Gradient-based learning applied to document recognition. *Proceedings of the IEEE*, 86(11):2278–2324, 1998a.
- LeCun, Y., Cortes, C., and Burges, C. Mnist dataset, 1998b.
- Liang, S., Li, Y., and Srikant, R. Enhancing the reliability of out-of-distribution image detection in neural networks. *arXiv preprint arXiv:1706.02690*, 2017.
- Louizos, C. and Welling, M. Structured and efficient variational deep learning with matrix gaussian posteriors. In *International Conference on Machine Learning*, pp. 1708–1716, 2016.
- MacKay, D. J. *Bayesian methods for adaptive models*. PhD thesis, California Institute of Technology, 1992.
- Naeini, M. P., Cooper, G., and Hauskrecht, M. Obtaining well calibrated probabilities using bayesian binning. In *Twenty-Ninth AAAI Conference on Artificial Intelligence*, 2015.
- Neal, R. M. *Bayesian learning for neural networks*, volume 118. Springer Science & Business Media, 2012.
- Netzer, Y., Wang, T., Coates, A., Bissacco, A., Wu, B., and Y Ng, A. Reading digits in natural images with unsupervised feature learning. *NIPS*, 01 2011.
- Niculescu-Mizil, A. and Caruana, R. Predicting good probabilities with supervised learning. In *Proceedings of the 22nd international conference on Machine learning*, pp. 625–632. ACM, 2005.
- Platt, J. et al. Probabilistic outputs for support vector machines and comparisons to regularized likelihood methods. *Advances in large margin classifiers*, 10(3):61–74, 1999.
- Simonyan, K. and Zisserman, A. Very deep convolutional networks for large-scale image recognition. *arXiv preprint arXiv:1409.1556*, 2014.
- Tschandl, P., Rosendahl, C., and Kittler, H. The ham10000 dataset, a large collection of multi-source dermatoscopic images of common pigmented skin lesions. *Scientific data*, 5:180161, 2018.

Zadrozny, B. and Elkan, C. Obtaining calibrated probability estimates from decision trees and naive bayesian classifiers. In *Icml*, volume 1, pp. 609–616. Citeseer, 2001.

Zadrozny, B. and Elkan, C. Transforming classifier scores into accurate multiclass probability estimates. In *Proceedings of the eighth ACM SIGKDD international conference on Knowledge discovery and data mining*, pp. 694–699. ACM, 2002.

Zagoruyko, S. and Komodakis, N. Wide residual networks. *arXiv preprint arXiv:1605.07146*, 2016.

A. Expected Calibration Error (ECE)

Another way to define calibration is based on the relation between the accuracy and confidence. Miscalibration can be interpreted as the difference between confidence and probability of correctly classifying a sample. For instance, in the case of a calibrated model, if we have the group of samples which has the confidence of $S_y(\mathbf{x}) = 0.9$, it is supposed to have 0.9 percentage of accuracy. Based on this definition of calibration, ECE is proposed as empirical expectation error between the accuracy and confidence (Naeini et al., 2015) in a range of confidence intervals. It is calculated by partitioning the range of confidence which is between $[0, 1]$ into L equally-spaced confidence bins and then assign the samples to each bin B_l where $l = \{1, \dots, L\}$ by their confidence range. Later it calculates the weighted absolute difference between the accuracy and confidence for each subset B_l . More specifically:

$$\text{ECE} = \sum_{l=1}^L \frac{|B_l|}{N} \left| \text{acc}(B_l) - \text{conf}(B_l) \right|, \quad (8)$$

where N is the total number of samples and $|B_l|$ is the number of samples fall in the interval B_l .

B. Implementation Specification of Skin Lesion Detection System

To test the impact of calibration in the real application, we design a medical assistant system. One of medical applications is anomaly detection for skin spots. We use ISIC dataset (Tschandl et al., 2018; Codella et al., 2017) which contains 10015 images of 7 different skin lesion types which are, Melanoma, Melanocytic nevus, Basal cell carcinoma (BCC), Bowen, Benign keratosis, Dermatofibroma, and Vascular. We select ResNet152 with pretrained weights on ImageNet as the classifier. In order to fine-tune it, we use 60% of ISIC images resizing them to 224×224 and normalizing with mean and standard deviation of the ImageNet dataset. Notice that we use stratification to divide the dataset.

We run the fine-tuning for 100 epochs with batchsize of 32 using Adam optimizer with starting learning rate of $1e-4$ and a scheduled decaying rate of 0.95 every 10 epochs. To increase the variety of the training samples, we perform data augmentation with probability of 0.5 of transforming every image with a random horizontal or vertical flip or a random rotation of a maximum of 12.5° either to the left or to the right. From the 40% of the data that we consider as the test samples, we select 20% of them as the validation which is 801 samples for calibration and hyper parameter tuning. We report the results on the rest of the test samples which are 3205.

C. More Results of Skin Lesion Detection System

In this section, we provide more results of skin lesion detection system. The confidence of the system before and after calibration by UTS method for correctly classified and misclassified samples is reported in Figure 3 for different skin lesion types. The temperature and calibration error of the trained model is reported in Table 2.

Unsupervised Temperature Scaling

Table 2. Comparing calibrating ResNet152 model trained on ISIC dataset with UTS approach.

Model	Dataset	ACC	Uncalibrated		UTS		T_{UTS}
			NLL	ECE%	NLL	ECE%	
ResNet152	ISIC	88.02%	0.712	0.092	0.461	0.068	1.712



Figure 3. Different correctly classified and misclassified output of skin lesion detection system before and after calibration with UTS.